Bridge Maintenance, Safety, Management and Life-Cycle Optimization – Frangopol, Sause & Kusko (eds)

Static and dynamic model validation and damage detection using wireless sensor network

S. Dorvash, R. Yao, S. Pakzad & K. Okaly
Lehigh University, Bethlehem, PA, USA

ABSTRACT: Recently, technological advances in wireless sensor network (WSN) have made structural health monitoring SHM more affordable and easier for implementation. Despite all advantages of WSN, due to lack of real experiments on its application in SHM and a few other challenging issues, this technology has not approached its wide-spread deployment. This paper presents an experimental work on a 3-D steel truss structure using WSN. Static tests are conducted to validate the properties of the structure and then dynamic test is used for extracting of modal properties and model updating of the system. Finally a local damage is simulated on the structure and two statistical approaches are employed to detect the structural change.

1 INTRODUCTION

As aging of bridge structures adversely affect their performance, technical strategies and damage detection algorithms are needed for their maintenance and safety considerations. Structural Health Monitoring (SHM), as a promising approach, addresses this issue. Monitoring of the state of a structure enables drawing the deterioration trend over its lifetime and detecting damage at its early stages. When, according to the report by the Federal Highway Administration (FHWA 2008), 27.6 % of bridges in United State are classified as structurally deficient and functionality obsolete, the outcome of SHM becomes more critically important for the maintenance and safety of bridges and highways. Hence, a great amount of researches has been focused on this area, over the past decade.

Traditionally, SHM has been developed based on the wired sensor network and central depository of data. While, the high cost and the installation difficulties associated with the wired sensor network have limited the large-scale application of sensor based SHM, technological advances in wireless sensor network (WSN) have made it more affordable and potentially scalable. As a result of these advantages, in some recent real-world SHM projects, WSN is selected as a primary data acquisition system. Wang et al., (2005), implemented 21 sensor nodes distributed over the main balcony of a historic theatre. Pakzad et al. (2008, 2009) presented the deployment of a large scale WSN including 64 sensing nodes along a bridge structure. Whelan et al. (2008) deployed a WSN consisting of 40 measurement channels from 20 sensing nodes. These examples show the researcher's interest in using WSN in SHM during the past few years.

Despite advantages of WSN, as any recently developed approach, it needs to be adequately verified under different real circumstances. Experimental implementation of an identification and damage detection algorithm using WSN is a promising way to evaluate the performance of this approach.

This paper presents an experimental implementation of a system identification and damage detection algorithm on a 3 dimensional steel truss using a recently developed WSN platform. The Imote2, developed by Intel, together with SHM-A sensor board, developed at University of Illinois (Rice et al. 2008), are main components of the WSN platform used in this experiment.

An analytical model of the truss structure is developed based on the available specification and the properties derived from static tests. Dynamic test is performed on the truss to estimate the modal properties using subspace state space algorithm (Overschee et al. 1994). Finally, local damage is simulated on the structure by adding additional weight at the midspan of the truss. Two unsupervised statistical damage detection algorithms are employed to separate the damaged signals from undamaged signals. The first one is statistical process control for damage-sensitive features (AR residuals), which is based on the premise that damage will significantly alter its statistical distribution; the other one is randomness tests of the features, where the Ljung-Box (Ljung et al. 1978) statistic is employed as the damage index and the critical threshold is established at the point above which the theoretical probability is smaller than a certain value.

2 WIRELESS SENSOR PLATFORM

Imote2, developed by Intel, is used as the hardware platform of this experiment. This platform contains Intel PXA271 CPU which has the ability of operation in low voltage (0.85V), low frequency (13MHz) mode. This feature provides very low power operation of the CPU. The processor's frequency can also be scaled from 13MHz to 416 MHz with dynamic voltage scaling which enables optimizing the power consumption. This platform also includes 256kB SRAM, 32 MB SDRAM and 32MB of FLASH memory which is distinguishable in compare with other smart sensor platforms.

Imote2 integrates CC2420 IEEE 802.15.4 radio transceiver from Texas Instruments which supports a 250kb/s data rate with 16 channels in the 2.4GHz band. A 2.4GHz surface mount antenna is provided on the Imote2 platform. To enhance the communication reliability, an external antenna, Antenova Titanis 2.4 GHz Swivel SMA, is used in addition to Imote2's onboard antenna. Table 1 presents the general specifications of the Imote2 platform.

Table 1, Specifications of Imote2

Parameter	Value
Processor	Intel PXA271
SRAM Memory	256kB
SDRAM Memory	32MB
FLASH Memory	32MB
Power Consumption	44mW at 13MHz 570mW at 416 MHz
Radio Frequency Band	2400.0 – 2483.5MHz
Dimensions	36mm×48mm×9mm

The Imote2 has many I/O options which make this platform flexible to operate with different sensor boards. Since the quality of the collected data entirely depends on the components of the sensor board, careful consideration should be given to selection of this element. The sensor unite of this experiment is SHM-A sensor boards, developed by Rice et al. (2008) in Smart Structures Technology Laboratory at Illinois University. Components of this unit are selected specifically for SHM applications. LIS3L02AS4 analog accelerometer manufactured by ST Microelectronics is used for SHM-A sensor board. LIS3L02AS4 is a low-cost, high sensitivity analog accelerometer with 50µg/√Hz Noise density which offers 3-axes of acceleration on one chip. Table 2 presents the specifications of this accelerometer. Low-pass filter, Gain difference amplifier and Quickfilter 16-bit ADC are other components integrated on the sensor board. The Quickfilter QF4A512 Programmble signal conditioner is the key component of SHM_A sensor board (Rice et. al. 2008). It utilizes 4-channels with 16-bit resolution ADC which provides a reasonable sensitivity for most of SHM purposes. Figure 1 shows a unit of sensor boards and Imote2.

Table 2, Specifications of LIS3L02AS4 Accelerometer

Parameter	Value
Acceleration Range	±2g
Avg. Noise Floor (X & Y)	0.3mg
Avg. Noise Floor (Z)	0.7mg
Resolution	0.66 V/g
Temperature Range	-40 to 85ºC

Software platform, as well as hardware platform, has an important role in the performance of a WSN. TinyOS operating system is the main framework for programming the Imote2. This operating system is an open source, component oriented software which supports a wide range of WSN's applications. In addition, there is a need for some high-level components to cooperate with the framework and maintain the specific requirements of SHM. The Illinois Structural Health Monitoring Project (ISHMP) has developed a software package that works with TinyOS for SHM applications. This is a package of applications satisfying the requirements for reliable monitoring of civil infrastructures. Remote Sensing application of ISHMP is used for data collection of this experiment. Two essential protocols in wireless data collection and transmission are time synchronization and reliable data transfer which both are employed in this program.

Figure 1, SHM-A Sensor board attached on the Imote2 Platform.

3 STATIC VALIDATION OF THE STRUCTURE

A challenging task in experimental works is validation of structural model using data from the structure. Generally, the response of the structure during the experiment is different from the expected behavior because of the nature of the structures and construction process. Static validation of structural properties based on analytical model is a solution to this problem. This section describes the static tests which are performed in order to validate the

Figure 2, 3-D steel truss of the experiment

structural properties of the truss. Figure 2 shows the truss structure used in the experiment.

The major task in static validation of structure is calibration of its material and geometric properties. For the simple 3-D truss, the unknown parameters are the properties of elements and the behavior of connections. Some of these parameters such as sectional properties could be easily obtained. Using these properties along with an initial estimated value for the modulus of elasticity the analytical model is built in the SAP2000.

To obtain an accurate value for the modulus of elasticity, deflections from the truss were compared with deflections in the analytical model under the same loading conditions. Ten loading configurations were set one-by-one on the truss while the vertical displacements were recorded at three different nodes. As an example, loading configuration 10 is shown in the figure 3. On the east elevation of the truss the three sensors were placed on the bottom three center nodes named "South," "Middle," and "North," respectively. In each of the ten configurations, all loads were placed on the east side of the truss. Each time the loadings are held in place long enough for the measurement systems to record many points, where the average is then taken. From these 10 configurations with three sensors, 30 points of deflection are obtained. These same loadings were applied to the analytical model, and the deflections at the three sensor locations were recorded. The actual deflections were compared with the analytical model. Linear regression is used to find a best estimate for the modulus of elasticity.

When comparing the relative error between actual and analytical model's deflections in all 30 points, it is found that some of the configurations had a much higher relative error than others, which could be the result of the following 2 facts: 1) some tests were held for a longer time, resulting in more samples than others, which in turn result in a more accurate

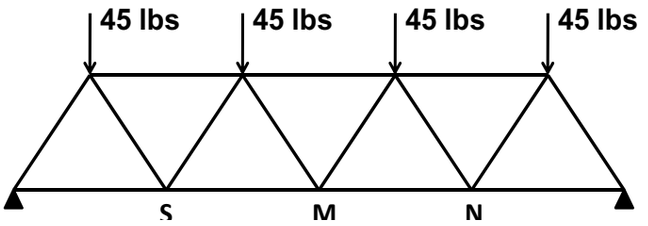

Figure 3, Loading configuration 10.

estimation. 2) The model error, specifically the connection stiffness, affects the estimation accuracy for some tests.

Finally the axial stiffness of elements in the SAP2000 model is adjusted with the result from above, which was 1244 kips.

4 DYNAMIC VALIDATION

4.1 *Extraction of Modal Properties*

In this section the modal properties of the truss including natural frequencies, damping ratios and mode shapes are estimated using dynamic test. Fourteen sensor nodes were attached to the joints of the truss to measure the dynamic response of the structure. Each sensor provides two set of acceleration data in two directions. The dynamic excitation is ambient and therefore stochastic identification method is used to derive the modal properties.

An additional sensor node is fixed on the ground as a reference node to represent the sensor and environmental noise characteristics. Using 280 Hz sampling frequency, data from the reference node and one of the sensors attached to the truss are collected. Figure 4 shows the time-history and the power spectral density (PSD) of the output from these two sensors. Comparison of the two signals in time domain shows that the signal to noise ratio of the collected data from the node on the structure is relatively large, making extraction of the structure's modal properties possible. In addition, inspection on PSD of two signals provides information about frequency content of the noise, in the measured accelerations. This knowledge is useful in realization of dynamic properties of the truss.

Figure 4 indicates that there are few dominant frequencies in the signal from the reference node which are possibly repeated in all the signals from structure's response. Two major sources of these frequency contents of the reference node are: modal properties of laboratory structure which correspond to approximately 7 and 17 Hz frequencies in PSD and the electrical devices in the experiment's environment which correspond to 60~65 Hz frequency range. Based on this realization, these frequencies should not be considered in the identification of truss's modal properties.

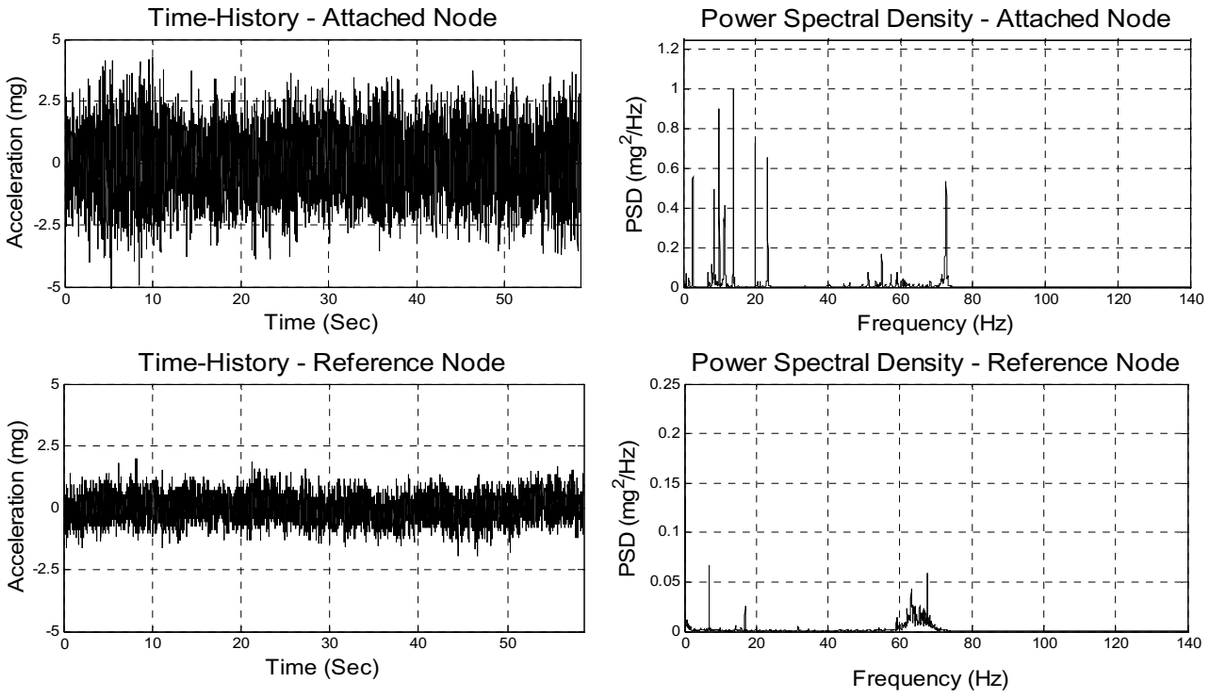

Figure 4, Comparison of the Outputs of Reference and Attached Nodes in Time and Frequency Domains

Dynamic tests were performed a few times to collect satisfactory data for identification purpose. Neglecting longitudinal response of the truss, totally 28 channels provided the acceleration data of the 14 joints of structure in two transverse directions. A low-pass digital filter with 35 Hz cut-off frequency is applied to the raw data to remove high frequency responses, which are not of major importance and also are more affected by noise. Afterward, Subspace state space algorithm is applied to the data to estimate the discrete-time state space model of the structure.

Stability diagram is used to determine the optimal model order for the system identification algorithm. Figure 5 shows this diagram for a limited frequency band-width which contains the major modes of the structure. The convergence tolerance for both frequency and damping ratio is 5%. The modal assurance criterion (MAC) is also used to check the convergence of the mode shapes in different model orders. This criterion is defined as below:

$$MAC_i = \frac{(\phi_i^T \times \phi_{i-1})^2}{(\phi_i^T \times \phi_i) \times (\phi_{i-1}^T \times \phi_{i-1})} \qquad (1)$$

where Φ_i and Φ_{i-1} are mode shape vectors of each mode calculated from state-space models with orders i-1 and i. The mode shapes are considered to be converged when MAC factor is greater than 0.95.

The stable model order is used for extraction of modal properties. As the reference node showed, there are some non-structural modal frequencies in the result that are removed from consideration. Additionally, the result of modal analysis of the numerical model gives information about the truss's frequencies and modal properties which helps realizing structural modes from the outputs of the algorithm.

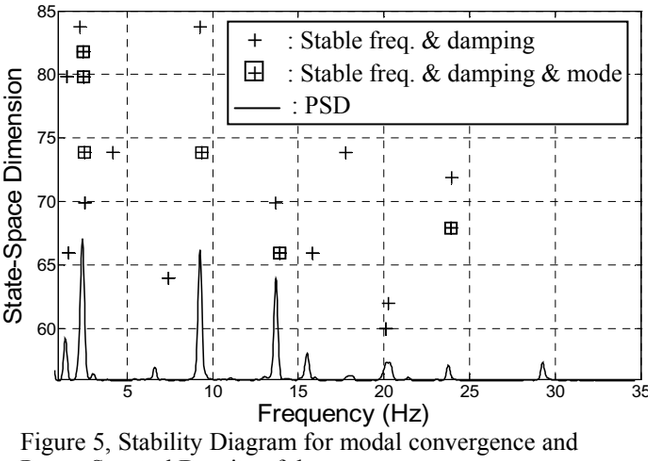

Figure 5, Stability Diagram for modal convergence and Power Spectral Density of the response.

First three mode shapes of the structure are presented in figure 6. It is observed that the first mode, which is significantly dominant, happens in the out-of-plane direction of the truss. This is also in agreement with the modal analysis of the analytical model.

As one of the aspects of this research, the developed analytical model is updated based on the results of dynamic test. Originally, there was a difference between frequencies of two analytical and experimental models which should be matched after model updating task. The most questionable parameter in the analytical model is the assumed boundary conditions. In fact, when the geometry and sectional properties of the structural members are known, boundary conditions are the major uncertain parame-

ters which influence the dynamic behavior of the system. For this reason, the end fixity, as a portion of the element's stiffness ($\alpha EI/l$), is defined as the variable to be determined by matching the frequencies. Another consideration remains for the consistency of updated model with the result of static test. Therefore, an iteration process between the modal and static analysis of the model is performed.

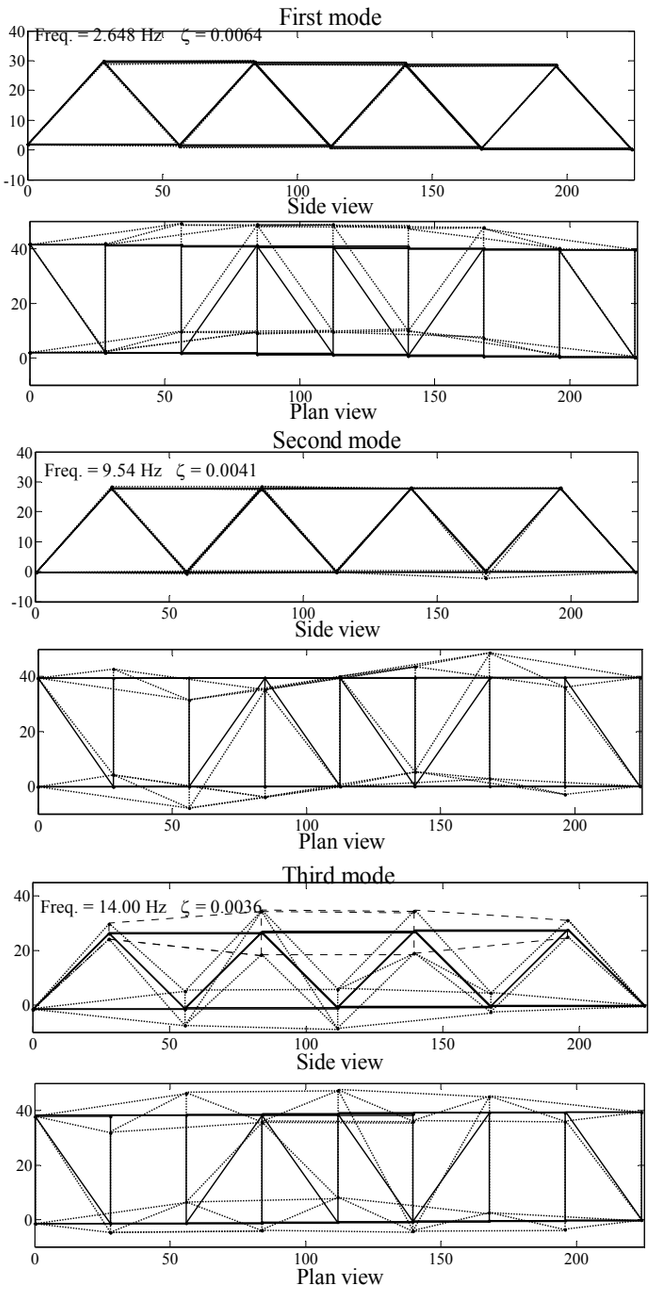

Figure 6, First 3 extracted mode shapes, frequencies and damping ratios.

Figure 7, shows the comparison of first mode shape obtained from both system identification and the updated analytical model.

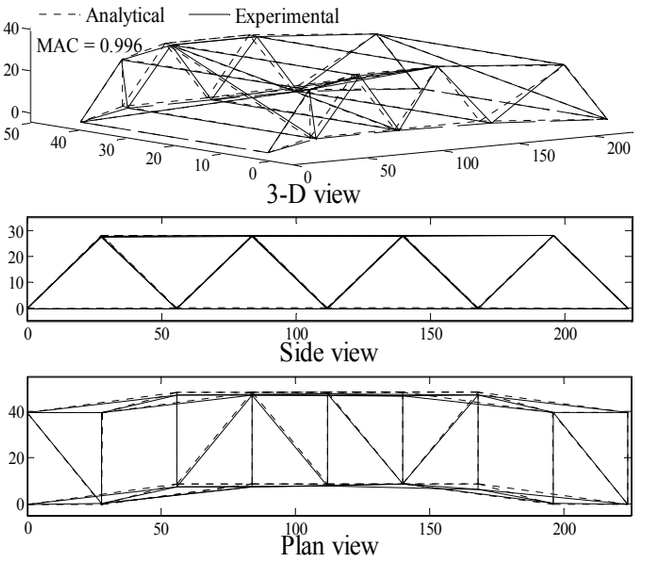

Figure 7, first mode shape: experimental vs. analytical result

5 DAMAGE DETECTION USING AUTO-REGRESSIVE MODEL

Given a time series x(t) (in this case acceleration measurements), an AR model with order p can be constructed as:

$$x(t) = \sum_{j=1}^{N} \alpha_j x(t-j) + e(t) \qquad (2)$$

where α_js are the model coefficients and $e(t)$ is random error. Once established, the model can be used to predict other time-series, and residuals are obtained as the error between prediction and real signal at different time points.

As long as the new measurements are similar to the baseline measurements to which this model is fitted, the prediction from the model should be close to new signal. However, if the incoming data is not acquired from the same structural condition under which baseline measurements are collected, then the model will no longer be able to make precise prediction, and a substantial change in the distribution of residuals is expected. Based on this reason, all the damage detection procedures discussed in this paper are focused on the analysis of residuals.

5.1 *Model Order Selection*

Akaike's Information Criterion (AIC) (Brockwell et al. 2002) is employed to select the proper model order. Its aim is to obtain a balance between the complexity of the model and accuracy of the prediction. According to this theory, the best model should be the one that minimizes the *AIC* value, which is the sum of the prediction error and a penalty term that increases with the number of parameters in the model.

Through AIC value comparison, the model order for this study is set at 28 lags. A series of trials also proved that higher order models do not yield a better performance.

5.2 *Statistical Damage Classification*

Damage is simulated by adding two 45-lb weight discs at the mid-span on the lower cord of the truss. Free vibration tests are conducted for both damaged and undamaged states; for each case two sets of acceleration measurements are collected by the WSN. In each case, system vibration is introduced by pushing the structure from mid-span and then releasing it when the sensors start recording data. A low-pass Chebyshev filter with cutoff frequency of 40 Hz is applied to the data. The sampling rate after filtering is 80Hz, and every data set contains 4250 samples.

5.2.1 *Statistical Process Control (SPC)*

Widely used in management of manufacture industries, SPC's underlying assumption is that when a system deviates from its original state, a change will occur in the statistical characteristics of the features monitored/charted. Generally, a control chart features a center line and two control limit lines (upper and lower bound).

Upper/Lower Control limits are drawn at points above/below which the likelihood for the features to occur is small. When the system is stable, the charted values should mostly remain inside the confidence region; otherwise, a significant amount of outliers will appear in the charts.

Only the last 2200 points of each data set is used here since the patterns shown by the first half are much affected by the initial load condition, which varies between different tests. The AR model is constructed using the first data set from undamaged state, and the other 3 are fitted to this model. The residual series (2200-28=2172 points) for all these four cases are then computed and divided into subgroups of size four, and control charts are used to detect the change in means and variances of residuals within each subgroup.

If the residuals are truly normally distributed random sequence, the subgroup mean should also have a normal distribution and the subgroup variance should have a chi-square distribution with degree of freedom three (Fugate et al. 2001). Hence, the control limits are $\pm z_{\alpha/2} s_p/\sqrt{n}$ for the mean $\bar{x}$ and $\bar{S}\sqrt{\chi^2_{1-\alpha/2,n-1}/(n-1)}$ and $\bar{S}\sqrt{\chi^2_{\alpha/2,n-1}/(n-1)}$, for standard deviation S, where $s_p/\bar{S}$ is the pooled variance/mean variance of baseline subgroups, α is the significance level (0.05 in this case) and n is the subgroup size.

The x-bar and S control charts, shown in Figures 8 & 9, are constructed from measurements at node 4.

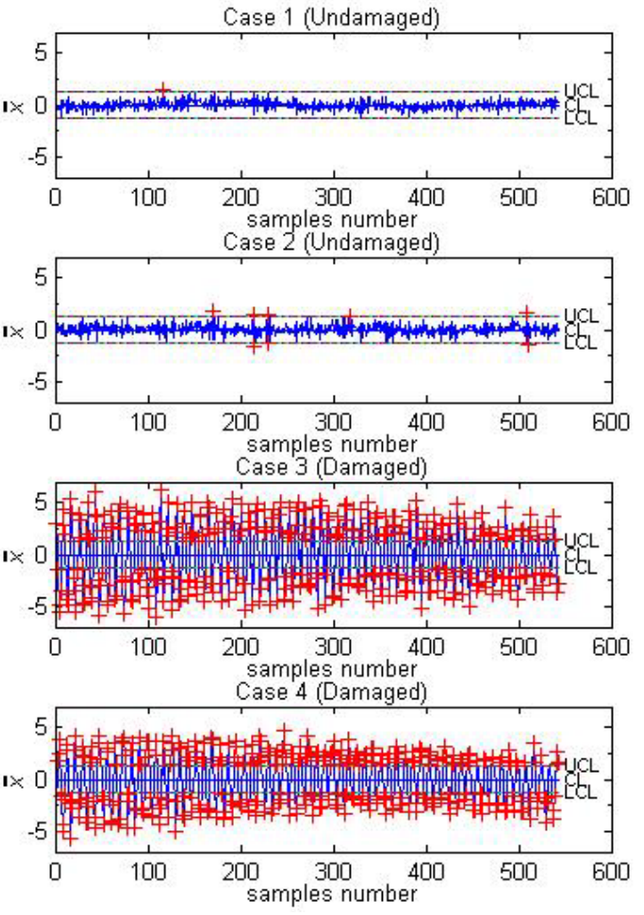

Figure 8, $\bar{x}$ control chart of the residuals

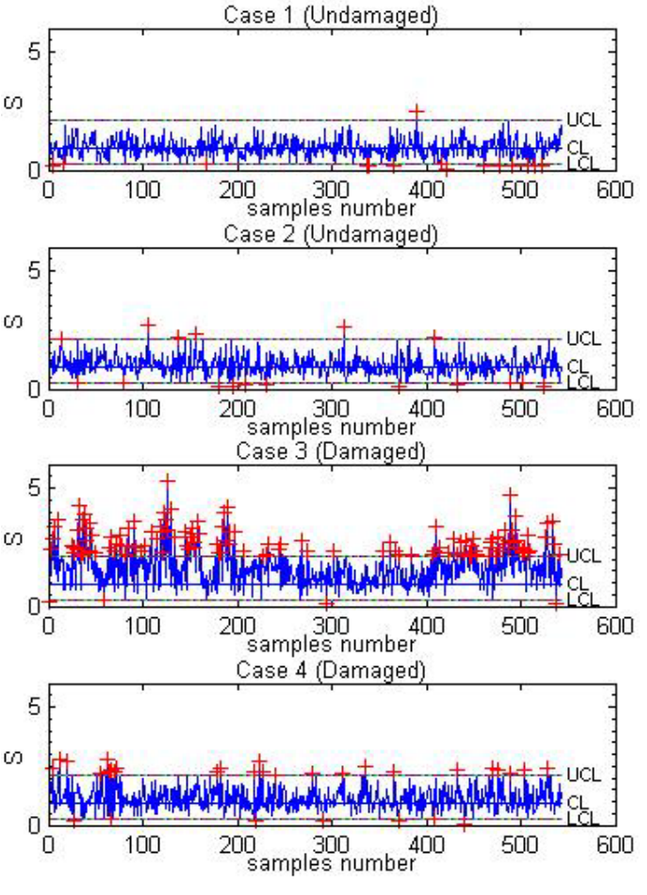

Figure 9, S control chart of the residuals

Investigation of all other nodes also yields similar results and thus is not presented here. It can be seen that the x-bar chart gives a better performance than S chart which is because of the fact that the system is still within the linear range, so the variance change in the residuals is not very significant.

5.2.2 *Randomness Test of Residuals:*

According to the definition of AR model, the residuals at different times should be nearly uncorrelated. In other words, if the model creates a good fit of the signal, then it should take care of everything predictable from information in the previous data, and the error should be the result of some random factors beyond control.

Therefore, when the model fails to make a good predication of the input, some information of the underlying signal generator will 'leak' into the residuals, thus creating patterns that can be detected using autocorrelation analysis.

The Ljung-Box test (Ljung et al., 1978) is a useful statistical tool to decide if the autocorrelation of a time series is near zero. Here H_0 (the null hypothesis) is that the signal is random. Extensively applied in autoregressive modeling, the test statistic is calculated by taking into consideration the autocorrelation value over a number of lags, and thus can well represent the overall randomness of a signal. Its definition is given in equation 3:

$$Q = n(n+2)\sum_{j=1}^{h}\frac{\rho_j^2}{n-j} \quad (3)$$

where n is the sample size or the length of the time series, h is the number of lags, and ρ_j is the autocorrelation at the jth lag. Since this Q statistic follows a χ^2 distribution under the normality assumption of the input, for a significance level α, the rejection threshold can be set at $\chi^2_{1-\alpha,h}$, which is the α-quantile of the χ^2 distribution with h degrees-of-freedom.

Three experiments are performed using this methodology. For all of the tests, α is equal to 0.05. In the first experiment, this test is applied to the whole length of each data set, and the lag number is selected to be 75. Measurements are all from node 4 as results from one node can fairly represent the overall behavior. One data set from undamaged state is used as the baseline to construct the AR model and the other is reserved for false-positive testing. In the second experiment, each data set is segmented into sixteen 500-sample blocks with 50% overlap, which are then labeled chronically from 1 to 16. On every 4 blocks with the same label but drawn from different files, a test can be conducted in the same way as in the first experiment, only with a reduced sample size, and hence a reduced lag number of 25. Signal 1 is used as the reference channel. The results from these two tests are summarized in tables 3 and 4.

Table 3. results from 1st experiment (measurements are taken from node 4)

	Hypothesis Testing result			
	1st test (Signal 1 as reference)		2nd test (Signal 2 as reference)	
	Q-statistic	H_0/H_1	Q-statistic	H_0/H_1
Signal 1: Undamaged	17.3895	0	50.8961	0
Signal 2: Undamaged	34.2123	0	21.3803	0
Signal 3: Damaged	1144.8	1	1094.3	1
Signal 4: Damaged	799.6384	1	962.7779	1

Table 4. results from 2nd experiment (number before the dash: times that H_0 is rejected; number after the dash: total number of tests)

Structural condition	Node num.				
	1	**2**	**3**	**4**	**5**
Signal 1:Undamaged	0/16	0/16	0/16	0/16	0/16
Signal 2:Undamaged	1/16	2/16	2/16	0/16	1/16
Signal 3:Damaged	16/16	16/16	16/16	16/16	16/16
Signal 4:Damaged	14/16	15/16	15/16	15/16	15/16
	6	**7**	**8**	**9**	**10**
Signal 1:Undamaged	0/16	0/16	0/16	0/16	0/16
Signal 2:Undamaged	0/16	2/16	2/16	1/16	1/16
Signal 3:Damaged	16/16	16/16	16/16	16/16	16/16
Signal 4:Damaged	15/16	16/16	15/16	16/16	15/16

Table 5. results from 3rd experiment

Structural Condition	Hypothesis Testing result	Test number (all signals come from node 4)			
		1	**2**	**3**	**4**
Signal 1: Undamaged	Q-statistic	2.49	2.07	2.25	2.19
	H_0/H_1	0	0	0	0
Signal 2: Undamaged	Q-statistic	4.10	6.84	14.77	7.93
	H_0/H_1	0	0	0	0
Signal 3: Damaged	Q-statistic	67.58	51.01	74.17	73.86
	H_0/H_1	1	1	1	1
Signal 4: Damaged	Q-statistic	80.17	55.97	69.97	51.76
	H_0/H_1	1	1	1	1
		5	**6**	**7**	**8**
Signal 1: Undamaged	Q-statistic	6.50	9.53	5.32	12.95
	H_0/H_1	0	0	0	0
Signal 2: Undamaged	Q-statistic	2.30	2.38	2.50	2.66
	H_0/H_1	0	0	0	0
Signal 3: Damaged	Q-statistic	90.70	41.31	51.49	65.42
	H_0/H_1	1	1	1	1
Signal 4: Damaged	Q-statistic	88.66	32.45	70.84	73.02
	H_0/H_1	1	0	1	1

Through examining the Q -statistics of the second experiment it is found that most cases of the misclassification happen in the tests of first few blocks, thus providing verification that data collected at the beginning of each case is not representative of the structural condition. The third experiment is carried out by taking eight random samples with size 500 out of the last half of every signal and performing

tests on them. The maximum time lag in *Q*-statistic calculation is again 25. For the first four tests the reference channel is signal 1, while for the last four the reference comes from signal 2. The algorithm's performance is nearly perfect, with only one misclassification. As shown in Table 5, the algorithm's performance is nearly perfect, with only one misclassification.

6 CONCLUSION

In this paper, static and dynamic tests were performed on an experimental 3D truss. Based on the specifications of the truss and the results of the static tests, an analytical model of the truss was developed. Using dynamic tests, modal properties of the structure were extracted and the analytical model was updated. As a result of dynamic updating, the fundamental vibration mode of the truss was matched with the analytical model.

Local damage was implemented on the structure and two damage detection algorithms, namely statistical process control and randomness test of AR residuals, were applied to detect the damage. Both algorithms give satisfactory performance. The randomness test of AR residuals presented a more acceptable result in the sense that it was less affected by excitation conditions and more sensitive to structural change. However, further validation tests are needed before a decisive conclusion can be reached regarding the effectiveness of these algorithms in general damage detection problems. Also, in the second method, the lag numbers were chosen in a somewhat arbitrary way. Further efforts are needed to quantify the relationship between the lag length and sample size. In general, the larger the sample size, the longer the lag.

7 ACKNOWLEDGEMENTS

The research described in this paper is supported by the National Science Foundation through Grant No. CMMI-0926898 by Sensors and Sensing Systems Program and Pennsylvania Infrastructure Technology Alliance (PITA) through Grant No. PIT-965-09. The authors thank Dr. Shih-Chi Liu for his support and encouragement.

8 REFERENCES

Brockwell, P. J., Davis, R.A. 2002. Introduction to Time Series and Forcasting, Second ed. Springer, NY.

Farrar, C. R., Duffey, T. A., Doebling, S. W., Nix, D. A. 1999. A Statistical Pattern Recognition Paradigm for Vibration-based Structural Health Monitoring, *2nd International Workshop on Structural Health Monitoring* ,Standford , CA.

Fugate, M. L., Sohn, H. and Farrar, C. R. 2001. Vibration-based Damage Detection Using Statistical Process Control, *Mechanical Systems and Signal Processing*. Vol. 15, No. 4, 707-721

Intel Corporation Research 2005. Intel Mote2 Overview, Version 3.0, Santa Clara, CA, Unite State.

ISHMP 2009. http://shm.cs.uiuc.edu/software.html

Ljung, G. M. and Box, G. E. P. 1978. On a Measure of Lack of Fit in Time Series Models ", *Biometrika,* Vol. 65, No.2, 297-303

Overschee, P. V. Moor, B. D. 1994. N4SID: Subspace Algorithms for the Identification of Combined Deterministic-Stochastic Systems. Automatica ISSN 0005-1098 CODEN ATCAA9 , vol. 30, no. 1, pp. 75-93.

Pakzad, S.N. 2010. Development and deployment of large scale wireless sensor network on a long-span bridge. *Smart Structures and Systems*, An International Journal, in press

Pakzad, S.N., and Fenves, G.L. 2009. Statistical analysis of vibration modes of a suspension bridge using spatially dense wireless sensor network. *ASCE Journal of Structural Engineering*, 135(7):863-872.

Pakzad, S.N., Fenves, G.L., Kim, S., and Culler, D.E. 2008. Design and Implementation of Scalable Wireless Sensor Network for Structural Monitoring. *ASCE Journal of Infrastructure Engineering,* 14(1):89-101.

Rice, J. and Spencer, B. F. 2008. Structural Health Monitoring sensor development for Imote2 Platform. *Sensors and Smart Structures Technologies for Civil, Mechanical, and Aerospace Systems*. San Diego, CA, USA, Vol. 6932, 693234.

Rice, J.A. and Spencer, B.F. 2009. Flexible Smart Sensor Framework for Autonomous Full-scale Structural Health Monitoring,. *NSEL Report Series*, No. 18, University of Illinois at Urbana-Champaign. (http://hdl.handle.net/2142/13635)

SAP2000 Educational Ver.14.1.0. 1976-2009. Structural Analysis Program, Computers & Structures, Inc. 1995, CA, United State.

Sohn, H., Farrar, C. R. 2001. Damage Diagnosis Using Time Series Analysis of Vibration Signals, *Smart Materials and Structures*, Vol.10, No 3, 446–452.

STMicroelectronics 2005. LIS3L02AS4 MEMS Inertial Sensor. Geneva, Switzerland.

TinyOS 2005. http://www.tinyos.net

U.S. department of transportation, 2008. Status of the Nation's Highways, Bridges and Transit: Conditions & Performance. *Report to Congress*, United State.

Wang, Y., Lynch, J. P. and Law, K. H. 2005. Validation of an integrated network system for real-time wireless monitoring of civil structures. *Proc. 5th Int'l Ws. Structural Health Monitoring*, Stanford, CA, September 12-14.

Whelan, M. J., Janoyan, K. D., 2009. Design of a Robust, High-rate Wireless Sensor Network for Static and Dynamic Structural Monitoring. *Journal of Intelligent Material Systems and Structures*, Vol. 20, No. 7, 849-863.